Waveguides in three-dimensional photonic bandgap materials for particle-accelerator on a chip architectures

Isabelle Staude,[1,5,*] Christopher McGuinness,[2,3,5] Andreas Frölich,[1] Robert L. Byer,[2] Eric Colby,[3] and Martin Wegener[1,4]

[1]*Institut für Angewandte Physik and DFG-Center for Functional Nanostructures (CFN), Karlsruhe Institute of Technology (KIT), Wolfgang-Gaede-Straße 1, D-76131 Karlsruhe, Germany*
[2]*Ginzton Labs, Nano Center, 348 Via Pueblo Mall, Stanford, California 94305, USA*
[3]*SLAC National Accelerator Laboratory, Menlo Park, California 94025, USA*
[4]*Institut für Nanotechnologie, Karlsruhe Institute of Technology (KIT), D-76021 Karlsruhe, Germany*
[5]*These authors have contributed equally to this work.*
[*]*ips124@physics.anu.edu.au*

Abstract: The quest for less costly and more compact high-energy particle accelerators makes research on alternative acceleration mechanisms an important enterprise. From the multitude of suggested concepts, the photonic accelerator design by B. M. Cowan [Phys. Rev. ST Accel. Beams **11**, 011301 (2008)] stands out by its distinct potential of creating an accelerator on a chip [Proposal E-163, SLAC (2001)]. Herein, electrons are accelerated by the axial electric field of a strongly confined optical mode of an air waveguide within a silicon-based three-dimensional photonic band-gap material. Using a combination of direct laser writing and silicon double inversion, we here present the first experimental realization of this complex structure. Optical spectroscopy provides unambiguous evidence for the existence of an accelerating waveguide mode with axial polarization.

©2012 Optical Society of America

OCIS codes: (160.5293) Photonic bandgap materials; (130.5296) Photonic crystal waveguides.

References and links

1. S. John, "Strong Localization of Photons in Certain Disordered Dielectric Superlattices," Phys. Rev. Lett. **58**(23), 2486–2489 (1987).
2. E. Yablonovitch, "Inhibited Spontaneous Emission in Solid-State Physics and Electronics," Phys. Rev. Lett. **58**(20), 2059–2062 (1987).
3. Z.-Y. Li and K. M. Ho, "Waveguides in three-dimensional layer-by-layer photonic crystals," J. Opt. Soc. Am. B **20**(5), 801–809 (2003).
4. X. E. Lin, "Photonic band gap fiber accelerator," Phys. Rev. ST Accel. Beams **4**(5), 051301 (2001).
5. R. H. Siemann, "Energy efficiency of laser driven, structure based accelerators," Phys. Rev. ST Accel. Beams **7**(6), 061303 (2004).
6. B. M. Cowan, "Three-dimensional dielectric photonic crystal structures for laser-driven acceleration," Phys. Rev. ST Accel. Beams **11**(1), 011301 (2008).
7. K. M. Ho, C. T. Chan, C. M. Soukoulis, R. Biswas, and M. Sigalas, "Photonic band gaps in three dimensions: New layer-by-layer periodic structures," Solid State Commun. **89**(5), 413–416 (1994).
8. C. Sears, E. Colby, R. Ischebeck, C. McGuinness, J. Nelson, R. Noble, R. Siemann, J. Spencer, D. Walz, T. Plettner, and R. Byer, "Production and characterization of attosecond electron bunch trains," Phys. Rev. ST Accel. Beams **11**(6), 061301 (2008).
9. C. M. S. Sears, E. Colby, R. J. England, R. Ischebeck, C. McGuinness, J. Nelson, R. Noble, R. H. Siemann, J. Spencer, D. Walz, T. Plettner, and R. L. Byer, "Phase stable net acceleration of electrons from a two-stage optical accelerator," Phys. Rev. ST Accel. Beams **11**(10), 101301 (2008).
10. M. Mero, J. Liu, W. Rudolph, D. Ristau, and K. Starke, "Scaling laws of femtosecond laser pulse induced breakdown in oxide films," Phys. Rev. B **71**(11), 115109 (2005).
11. K. Soong, R. L. Byer, C. McGuinness, E. Peralta, and E. R. Colby, "Experimental Determination of Damage Threshold Characteristics of IR Compatible Optical Materials," in *Proceedings of Particle Accelerator Conference 2011*, (2011) pp. 277–279.
12. M. Deubel, G. von Freymann, M. Wegener, S. Pereira, K. Busch, and C. M. Soukoulis, "Direct laser writing of three-dimensional photonic-crystal templates for telecommunications," Nat. Mater. **3**(7), 444–447 (2004).

#160222 - $15.00 USD
Received 20 Dec 2011; accepted 11 Jan 2012; published 22 Feb 2012
(C) 2012 OSA

13. N. Tétreault, G. von Freymann, M. Deubel, M. Hermatschweiler, F. Pérez-Willard, S. John, M. Wegener, and G. A. Ozin, "New Route to Three-Dimensional Photonic Bandgap Materials: Silicon Double Inversion of Polymer Templates," Adv. Mater. **18**(4), 457–460 (2006).
14. I. Staude, M. Thiel, S. Essig, C. Wolff, K. Busch, G. von Freymann, and M. Wegener, "Fabrication and characterization of silicon woodpile photonic crystals with a complete bandgap at telecom wavelengths," Opt. Lett. **35**(7), 1094–1096 (2010).
15. I. Staude, G. von Freymann, S. Essig, K. Busch, and M. Wegener, "Waveguides in three-dimensional photonic-band-gap materials by direct laser writing and silicon double inversion," Opt. Lett. **36**(1), 67–69 (2011).
16. C. McGuinness, E. R. Colby, and R. L. Byer, "Accelerating electrons with lasers and photonic crystals," J. Mod. Opt. **56**(18-19), 2142–2147 (2009).
17. V. Lujala, J. Skarp, M. Tammenmaa, and T. Suntola, "Atomic layer epitaxy growth of doped zinc oxide thin films from organometals," Appl. Surf. Sci. **82–83**, 34–40 (1994).
18. A. Frölich and M. Wegener, "Spectroscopic characterization of highly doped ZnO films grown by atomic-layer deposition for three-dimensional infrared metamaterials," Opt. Mater. Express **1**(5), 883–889 (2011).
19. S. Rinne, F. García-Santamaría, and P. V. Braun, "Embedded cavities and waveguides in three-dimensional silicon photonic crystals," Nat. Photonics **2**(1), 52–56 (2008).
20. S. Kawashima, K. Ishizaki, and S. Noda, "Light propagation in three-dimensional photonic crystals," Opt. Express **18**(1), 386–392 (2010).
21. S. G. Johnson and J. D. Joannopoulos, "Block-iterative frequency-domain methods for Maxwell's equations in a planewave basis," Opt. Express **8**(3), 173–190 (2001).
22. C. D. Barnes, R. L. Byer, E. R. Colby, B. M. Cowan, R. J. Noble, D. T. Palmer, T. Plettner, R. H. Siemann, J. Spencer, and D. Walz, "Laser Acceleration of Electrons in Vacuum," Proposal E-163, SLAC (2001). **http://www-project.slac.stanford.edu/E163/E163ProposalClean.pdf**

1. Introduction

Waveguide architectures in three-dimensional photonic band-gap materials are usually discussed in the context of integrated optics, where they may be used to connect different components on a photonic chip [1–3]. Yet, they might also lead to applications in a completely different field, namely laser-driven acceleration of charged particles, thereby making use of the extraordinary electric fields and efficiencies provided by laser systems [4, 5].

In this work we follow the theoretical proposal by B. M. Cowan [6], which is based on a specifically engineered waveguide geometry inside a three-dimensional silicon photonic-crystal structure based on the woodpile geometry [7]. A sketch of the structure geometry as adjusted to our experimental conditions is depicted in Fig. 1(a). In contrast to the usual woodpile geometry, the host structure is made vertically symmetric by inverting the upper half of the lattice. This symmetry reduces deflecting field components in the accelerating mode [6]. Inside of this host structure, a waveguide is formed by removing all dielectric material in a region extending over the entire length of the structure in the particle-beam propagation direction z. Importantly, this waveguide supports transverse magnetic modes (TM) with the electric-field vector pointing in waveguide direction, such that the longitudinal electric field can impart energy onto charged particles moving along the waveguide. The mode profile of one of these modes is shown in Fig. 1(b). Adjustment of the exact length of the central rods extending into the waveguide, which are marked by the red circles in Fig. 1(a), will ultimately allow one to control the strength of the quadrupole moment of the waveguide mode, making it possible to optimize it either for electron acceleration or focusing [6]. While different charged particles may be accelerated along these lines, we will speak about electrons only in what follows.

The structure is designed to operate as a traveling-wave accelerator, where the electrons and the electric-field maxima move synchronously along the waveguide with the electrons staying at the peak of the accelerating phase at all times as schematically shown in Fig. 1(c). To make this possible, the electrons are assumed to arrive in trains of short bunches spaced by the wavelength λ of the accelerating mode [8, 9], in much the same way bunch trains are accelerated in RF accelerators.

#160222 - $15.00 USD Received 20 Dec 2011; accepted 11 Jan 2012; published 22 Feb 2012
(C) 2012 OSA

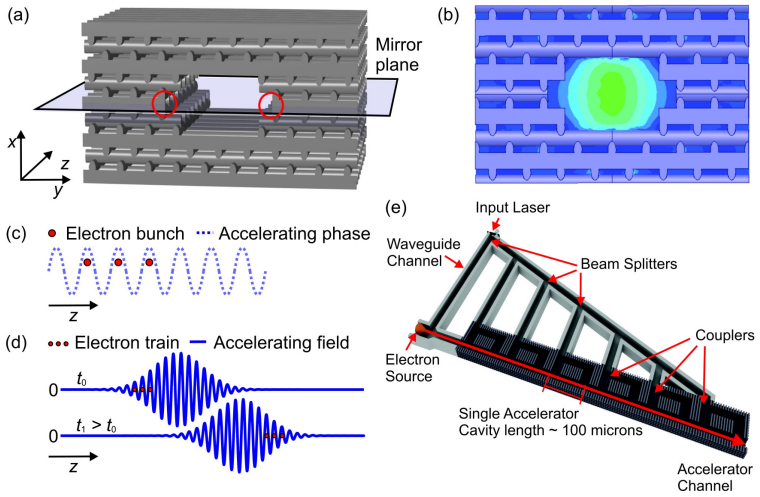

Fig. 1. Accelerating mechanism. (a) Design sketch of the waveguide geometry inside the woodpile based silicon structure [6]. (b) z-component of the electric field for the accelerating mode as seen by a speed-of-light particle. (c) Schematic of a train of electron bunches situated at the peaks of the accelerating phase. (d) Snap shots of the accelerating field and the particle bunch train at two different time steps (not to scale), if short laser pulses with $v_g < v_e \sim c$ are used to excite the accelerating mode. (e) Concept of a staged laser accelerator. Each cavity is powered by an external laser coupled into the cavity. A single laser pulse is split several times to power a series of cavities. For a 1 ps long laser pulse, and a group velocity of 0.26 × c, each cavity length is 105 µm. Image: Courtesy of Greg Stewart, SLAC.

The maximum accelerating gradient that can be obtained is limited by the optical damage threshold of the silicon structure. Damage fluence F_{th} for dielectric materials with permittivity ε has been shown to scale with pulse length τ as $\tau^{0.3}$ for pulse lengths below 1 ps at infrared wavelengths [10], while the peak electric field scales according to $E = \sqrt{2F_{th} / \varepsilon c \tau}$. Thus, in order to achieve high accelerating gradients short laser pulses have to be used to excite the waveguide mode for electron acceleration. Silicon has a damage fluence of 0.35 J/cm^2 for 1 ps long pulses at 2.2 µm [11], yielding a peak electric field of 469 MV/m for 1 ps pulses, and up to 1,048 MV/m when scaled to 100 fs pulses. For the mode depicted in Fig. 1(b), the ratio of the electric field on axis to the peak electric field in the medium is 0.18, resulting in a peak electric field for acceleration of 84 MV/m for 1 ps pulses, and even 189 MV/m for 100 fs pulses in silicon.

The pulse length in turn determines the effective length of an accelerating cavity. The group velocity for the mode depicted in Fig. 1(b) is v_g = 0.26 × c. Assuming the electron bunch train is fully relativistic, it will outrun the laser pulse by $\tau = L/c\,(1-\beta_g)/\beta_g$ [6], where $\beta_g = v_g$/c, as illustrated in Fig. 1(d). Therefore, the ultimate accelerator will consist of a series of short cavities staged sequentially as depicted in Fig. 1(e). For a 1 ps long pulse and group velocity of 0.26 × c the length of each cavity segment will be L = 105 µm.

2. Structure fabrication

For the fabrication of these rather complex structures we have used a combination of direct laser writing [12] and silicon double inversion [13, 14]. This overall approach is characterized by its high flexibility and makes even complicated structure geometries experimentally accessible [15]. Furthermore, the approach is inherently three-dimensional, thus allowing for the fabrication of many woodpile layers and sufficiently large structure footprints within reasonable time, in contrast to layer-by-layer approaches which are limited in the number of layers achievable [16]. For the direct laser writing (DLW) of polymer templates we have used a commercial instrument (Nanoscribe Photonic Professional) together with a commercial

#160222 - $15.00 USD
Received 20 Dec 2011; accepted 11 Jan 2012; published 22 Feb 2012
(C) 2012 OSA

negative-tone photoresist (IP-L from Nanoscribe GmbH). The waveguide is introduced into the host structure during the DLW process by switching off the writing laser when it passes over the waveguide region. The aspect ratio of the woodpile rod cross section has been adjusted by building up each rod by three individual exposures, which are laterally displaced by 65 nm with respect to each other [14]. Polymer shrinkage in the woodpile stacking direction has been pre-compensated by multiplication of all *x*-coordinate points in the control file with a factor of 1.3. Further effects of polymer shrinkage leading to distortion of the structure in the waveguide region have been alleviated by laterally displacing affected rods by empirical offsets of up to 225 nm. Aiming at a homogeneous filling fraction of the host structure in woodpile stacking direction, the writing laser power has been increased linearly by 9% from the bottom to the top of the structure. After direct laser writing a silicon replica of the photoresist templates is obtained *via* silicon double inversion [13, 14].

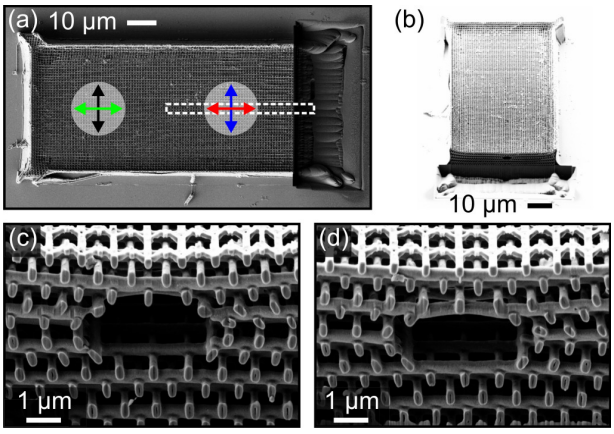

Fig. 2. Pilot sample of a photonic accelerator segment. (a) Top-view electron micrograph of a fabricated silicon structure. The waveguide position is marked by the dashed white lines. The two sampling areas for optical transmittance measurements in the waveguide region and in the reference area are highlighted by the white shaded circles. The colored arrows aim at connecting the sampling areas and the indicated polarizations of the incident electric fields to the measured spectra shown in Fig. 3(a) and (b). On the right hand side of the sample we have performed focused ion beam (FIB) milling in order to reveal the waveguide buried inside. (b) Oblique-view electron micrograph of the same sample looking at the FIB cross section with the waveguide opening at its centre. (c) and (d) Close-ups of the waveguide opening for two different characteristic *z*-positions of the FIB-cut separated from each other by approximately half a rod distance.

We have observed that the large size of the target waveguide structure renders the host structure rather fragile by design during the inversion procedure. A crucial step to avoid deformations and, thus, to achieve a high structural and optical quality despite the given design is the appropriate choice of the intermediate material used during the silicon double inversion procedure. Here, we have chosen ZnO deposited *via* an atomic-layer-deposition process using a commercial instrument (Cambridge NanoTech Savannah 100) and diethylzinc and hydrogen peroxide as precursors [17, 18]. In contrast to the previously employed silica [13–15], the ZnO inverse structure shows no obvious shrinkage upon resist removal.

Scanning electron micrographs of a typical sample fabricated along these lines are depicted in Fig. 2. The total length of the sample measures approximately 100 µm, corresponding to the approximate length of a single accelerating cavity. The samples presented here are intentionally designed such that the waveguide extends only halfway

#160222 - $15.00 USD
Received 20 Dec 2011; accepted 11 Jan 2012; published 22 Feb 2012
(C) 2012 OSA

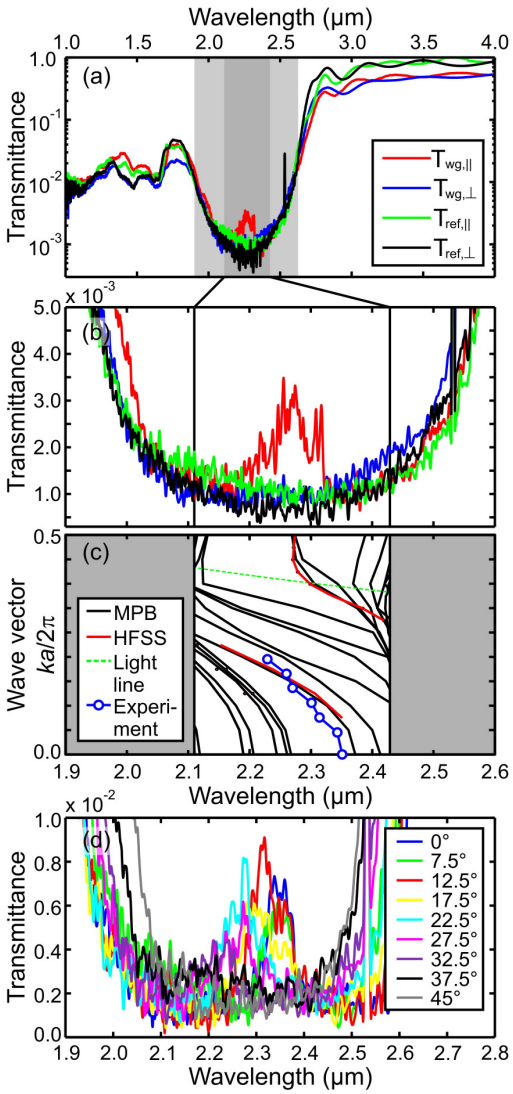

Fig. 3. Optical characterization of fabricated samples and comparison with theory. (a) Linear-optical transmittance spectra of the sample shown in Fig. 2, collected both in the waveguide region (wg) and in the undisturbed reference area (ref). In these measurements we have used linearly polarized light with the electric field oriented either parallel (∥) or perpendicular (⊥) to the waveguide. The position of the woodpile photonic stop band in spectroscopy direction calculated for experimental structure parameters is shaded in light gray, the calculated complete three-dimensional photonic band gap in dark gray. (b) Close-up of the measured data on a linear scale, clearly revealing the waveguide signature for longitudinally polarized incident light. (c) Numerical simulations: Dispersion diagram for a structure with parameters modeled after that depicted in Fig. 2. Black solid lines are MPB results. HFSS has been used for refined recalculation of the dispersion of the speed-of-light mode and of the mode existing at experimentally excitable *k*-values, showing excellent agreement with the MPB results. Also included in this panel are peak positions from the measurements shown in Fig. 3(d) (blue circles). (d) Angle-resolved transmittance spectra for a nominally identical sample.

through the structure, as indicated by the dashed lines in Fig. 2(a). This design allows us to perform optical transmittance measurements both in the waveguide region and, as controls, in an undisturbed reference area. The two corresponding sampling areas are schematically marked by the white shaded circular areas. In order to reveal the accelerating waveguide inside the structure, we have performed focused-ion-beam (FIB) milling. Figure 2(b) exhibits

#160222 - $15.00 USD
Received 20 Dec 2011; accepted 11 Jan 2012; published 22 Feb 2012
(C) 2012 OSA

an overview of the structure looking at the FIB cross section under oblique incidence. Close-ups of the waveguide opening for two different characteristic z-positions of the FIB-cut are presented in Figs. 2(c) and (d). These images demonstrate that recent progress in three-dimensional optical lithography and inversion techniques has indeed rendered these structures experimentally accessible – despite their structural complexity.

3. Polarization-resolved linear-optical transmission spectroscopy

In order to investigate the optical properties of the fabricated samples, polarization-resolved linear-optical transmittance spectra for the incident electric-field vector oriented parallel and perpendicular to the waveguide direction, respectively, have been recorded using a commercial Fourier-transform infrared microscope-spectrometer (Bruker Equinox 55, Opticon 36 × Cassegrain objective). Note that, due to the extreme fabrication challenge, up to now only extremely few measured waveguide signatures in complete photonic band-gap materials have been presented at near-infrared frequencies [15, 19, 20]. None of these would have been suitable for particle acceleration. Our results for the sample in Fig. 2 are depicted in Figs. 3(a) and (b). The most prominent feature present in these spectra is the photonic stop band in spectroscopy direction. Within the photonic stop band another distinct feature can be observed, but only for measurements in the waveguide region and for the linear polarization with the electric-field vector pointing in the waveguide direction (red curve), where accelerating waveguide modes are expected to couple to the incident light. We have been able to observe this characteristic longitudinally-polarized waveguide signature for a total of more than ten different fabricated samples.

In order to compare our experimental findings with theory we have performed numerical calculations for experimental structure parameters using both the freely available MIT-Photonic-Bands (MPB) Package [21] and the commercial finite element frequency domain simulation tool HFSS from ANSYS. Figure 3(c) shows the waveguide dispersion diagram for eigenmodes computed from these simulations. The field plot depicted in Fig. 1(b) has been obtained using HFSS. At 2.297 μm and $ka/2\pi = 0.392$ the TM mode that corresponds to this field plot crosses the light line, making it well suited for acceleration of fully relativistic particles. In the transmittance experiments, on the other hand, modes existing at smaller values of the wave vector k are detected, as determined by the range of incident angles of 15-30 degrees covered by the Cassegrain objective. For a more direct comparison with theory we have performed additional angle-resolved transmittance measurements by tilting the sample and reducing the range of incident angles to 0-7.5 degrees by an aperture. These results are depicted in Fig. 3(d) for a nominally identical sample. The positions of the peak maxima taken from smoothed experimental data for incident angles between 0 and 32.5 degrees are also included in Fig. 3(c). Good agreement exists with one of the modes found in the simulations, which we have checked to feature longitudinally polarized electric field components.

4. Conclusion

In conclusion, using commercially available tabletop optical-lithography technology we have experimentally realized and optically characterized pilot samples of three-dimensional photonic band-gap particle-accelerator segments. Our results represent an important first step towards approaching the goal, as stated by E. R. Colby et al. [22], "...to lithographically produce the power source, power transmission system, accelerator structures, and beam diagnostics on a single substrate by semiconductor process."

Acknowledgments

We acknowledge financial support provided by the Deutsche Forschungsgemeinschaft (DFG) and the State of Baden-Württemberg through the DFG-Center for Functional Nanostructures (CFN) within subproject A1.4. Funding is also provided by US Department of Energy contracts DE-AC02-76SF00515 and DE-FG03-97ER41043-II. The Ph.D. education of A.F. is embedded into the Karlsruhe School of Optics and Photonics.

#160222 - $15.00 USD Received 20 Dec 2011; accepted 11 Jan 2012; published 22 Feb 2012
(C) 2012 OSA